Calorimetric Study of Correlated Disordering in $[Hdamel]_2[Cu^{II}(tdpd)_2]\cdot 2THF$ Crystal

Yasuhisa Yamamura,[†] Hiroyasu Shimoi,[†] Masato Sumita,[†] Syuma Yasuzuka,[†] Keiichi Adachi,[‡] Akira Fuyuhiro,[‡] Satoshi Kawata,[‡] and Kazuya Saito*,[†]

Department of Chemistry, Graduate School of Pure and Applied Sciences, University of Tsukuba, Tsukuba, Ibaraki 305-8571, Japan and Department of Chemistry, Graduate School of Science, Osaka University, Toyonaka, Osaka 560-0043, Japan

Received: November 16, 2007; Revised Manuscript Received: February 14, 2008

The heat capacity of $[Hdamel]_2[Cu^{II}(tdpd)_2]\cdot 2THF$ was measured from 6 to 250 K by adiabatic calorimetry. There are four heat anomalies around 150 K associated with disordering in the orientation of the uncoordinated THF molecules and in the conformation of the out-of-plane allyl groups of $[Hdamel]^+$ units. The total entropy of transition was determined to be 19.8 J K^{-1} mol^{-1}, less than the $4R$ ln 2 (R = gas constant) expected from the crystal structure at room temperature. The smallness of the total entropy change on phase transitions proves the presence of the strong motional correlation between the adjacent allyl groups. The calorimetric conclusion agreed with the crystal structure at 200 K re-examined in this study.

I. Introduction

Metal complexes provide a great variety of structures that generate various physical properties and attract considerable attention for basic research and practical application.[1–20] The structures of the metal complexes are fundamentally composed of central metal cations, surrounding ligands, and uncoordinated molecules as a "spacer". The ligands and the uncoordinated molecules play the most important role in constructing the crystal structure of the complex, because these arrange the metal cations and adjust a distance between the cations, leading to a variety of physical properties of the complexes.[1–20] Thus, it is very important for rational design of new metal complexes to investigate the physical "properties" of the ligands and the uncoordinated molecules in complexes.

In metal complexes, it is well-known that the ligands and uncoordinated molecules present a variety of dynamics concerning translational, rotational, and intramolecular motional degrees of freedom. Dynamical properties of the ligands and the uncoordinated molecules in the complexes have been extensively investigated by structural and spectroscopic methods. Analyses are usually made within a one-particle scheme. On the other hand, we have pointed out that the motional correlation could be quantitatively evaluated through entropy change measured by calorimetry.[21–23] For example, $Pt_2(MeCS_2)_4I$, which is a mixed-valence binuclear one-dimensional MMX chain compound, shows an order−disorder phase transition associated with a concerted twist of "four" CS_2 moieties bridging two Pt atoms.[21] In this case, the motional correlation was clearly demonstrated through quantitative analysis of the entropy of transition. Although understanding the motional correlation is very important for the study of the metal complexes, the number of such studies is still limited to only a few.[21–23]

The title compound, $[Hdamel]_2[Cu^{II}(tdpd)_2]\cdot 2THF$,[24] belongs to a group of complexes assembled via multiple hydrogen-bonds, which have received considerable attention in the field of crystal engineering. This compound consists of mononuclear $[Cu(tdpd)_2]^{2-}$ dianions (Figure 1a), $[Hdamel]^+$ cations (Figure 1b), and uncoordinated THF molecules. One $[Cu(tdpd)_2]^{2-}$ anion and two $[Hdamel]^+$ cations form one building module through three hydrogen-bonds. The module is then linked to the adjacent modules also by hydrogen bonds to construct one-dimensional chains. There are two uncoordinated THF molecules per one building module. The one-dimensional chains are stacked and form a layered structure. One of the allyl groups of $[Hdamel]^+$ and the uncoordinated THF molecules are disordered orientationally over two positions at room temperature.[24] The previous differential scanning calorimetry (DSC) and structural studies[24] showed that the compound underwent a phase transition related to the orientational disorder around 155 K, below which a unit cell volume increased by a factor of 3 (at 140 K). The structural results suggested the existence of a strong correlation among the allyl groups of $[Hdamel]^+$ units and the uncoordinated THF molecules. Besides, considering the third law of thermodynamics, a phase transition and/or a glass transition will plausibly take place below 140 K. In this paper, the result of precise calorimetry on $[Hdamel]_2[Cu^{II}(tdpd)_2]\cdot 2THF$ is reported. The detailed analysis of the entropy of transition shows the motional correlation between adjacent allyl groups. Re-examination of the crystal structure yields the strength of the correlation as an energy diagram.

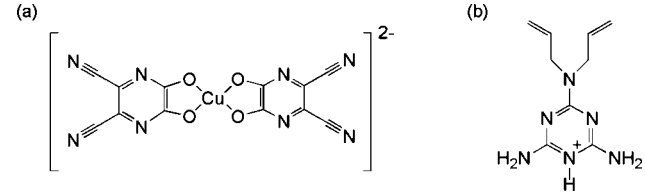

Figure 1. Structures of (a) $[Cu^{II}(tdpd)_2]^{2-}$ and (b) $[Hdamel]^+$.

II. Experimental Section

$[Hdamel]_2[Cu^{II}(tdpd)_2]\cdot 2THF$ was synthesized from solutions as described elsewhere.[24] The amount of THF in the sample for heat capacity measurement was ensured by thermogravimetry. The sample for calorimetry was sealed in a gold-plated copper calorimeter vessel with helium and saturated vapor of THF under atmospheric pressure. The mass of the sample was

* Corresponding author e-mail: kazuya@chem.tsukuba.ac.jp.
† University of Tsukuba.
‡ Osaka University.

10.1021/jp710936q CCC: $40.75
Published on Web 04/09/2008

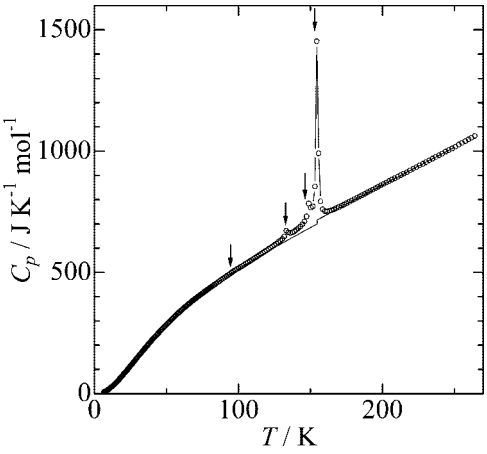

Figure 2. Heat capacity of $[Hdamel]_2[Cu^{II}(tdpd)_2]\cdot 2THF$. Arrows indicate the locations of heat anomalies. A solid line is a normal heat capacity to separate excess heat capacity.

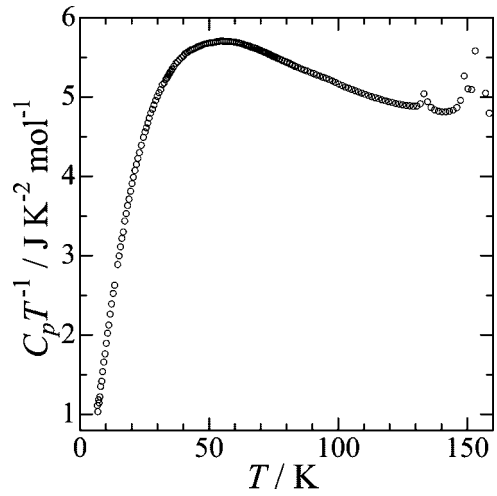

Figure 3. Heat capacity divided by temperature of $[Hdamel]_2[Cu^{II}(tdpd)_2]\cdot 2THF$.

2.7167 g (2.8826 mmol) after the buoyancy correction. The working thermometer mounted on the calorimeter vessel was a platinum resistance thermometer (Minco, S1059). Its temperature scale is based upon the ITS-90. The details of the adiabatic calorimeter used and its operations are described elsewhere.[25] The measurement was carried out by the so-called intermittent heating adiabatic method. The temperature increment by a single energy input (Joule heating) was less than 1% of the temperature. After energy input was turned off, thermal equilibrium inside the vessel was attained within a normal time (1–10 min depending on temperature) outside the temperature region near phase transitions. The sample contributed to heat capacity by 20% of the total heat capacity including that of the vessel at 50 K, 17% at 100 K, and 22% at 200 K. A suitable single crystal for X-ray crystallography was chosen and was mounted on a glass fiber with epoxy resin. X-ray measurement was carried out by a Rigaku/MSC Mercury CCD diffractometer with graphite-monochromated MoKα radiation. Data collection was performed at 200 K under flow of nitrogen gas for controlling the sample temperature. The structure was solved by direct methods (Rigaku Crystal Structure crystallographic software package of Molecular Structure Corporation) and refined with the full-matrix least squares technique (SHELEXL-97[26]).

III. Results and Discussion

Heat capacity (C_p) of $[Hdamel]_2[Cu^{II}(tdpd)_2]\cdot 2THF$ was measured below 250 K and is shown in Figure 2. The results show four heat anomalies in the temperature region from 80 to 210 K. The largest anomaly is seen at 155 K and corresponds to the anomaly in the previous DSC result.[24] The four anomalies are related to disordering in the conformation of the allyl group of $[Hdamel]^+$ and in the orientation of the uncoordinated THF molecules as shown later. Because supercooling was observed for each heat anomaly, all four heat anomalies are ascribed to phase transitions of the first order.

There is no anomaly associated with fusion of THF around its melting point (165 K). The excess THF is, thus, negligible in this experiment. To see details below 80 K, $C_pT^{-1} - T$ was plotted in Figure 3. The plot shows no anomaly below 80 K and indicates neither glass transition nor phase transition from 6 to 80 K. This implies that the disorders detected at room temperature are completely resolved below 80 K, in contrast to the suggestion in the previous work.[24]

To separate excess heat capacities, it is necessary to subtract the contribution of the intramolecular vibrational degrees of freedom (303 modes) and of the external lattice vibration (3 acoustic and 27 optical branches) and the so-called $C_p - C_v$ correction term from the total heat capacity.

The first contribution was estimated within an Einstein model based on vibrational data and a quantum chemical calculation. The intramolecular vibrational frequencies of THF were taken from the previous assignment,[27] except for the lowest frequency mode. The contribution of the lowest modes to heat capacity was determined by fitting with Einstein function as described below. The quantum chemical calculations were carried out for isolated ions of $[Hdamel]^+$ and $[Cu(tdpd)_2]^{2-}$; GAUSSIAN03[28] was used for this purpose. The molecular geometry was optimized under the DFT/B3LYP level using the LanL2DZ basis set. Vibrational analysis was then performed. Resultant frequencies obtained through such calculation usually deviate systematically from the experimental ones, and the deviation can be corrected for by multiplying by a correcting factor. Becuase the estimation of the second and third contributions need curve fitting, the correcting factor was included in a set of fitting parameters.

The contribution of the external lattice vibrations is assumed being described by Debye and Einstein models.[29] The degrees of freedom involved are 3 for the acoustic mode assuming a Debye model and are 27 for the optical branches assuming an Einstein model. Two lowest intramolecular modes of two THF molecules are also treated as optical modes. The $C_p - C_v$ correction is approximated by the Lindemann relation: $C_p - C_v \propto AC_pT^2$.

Because of the first order nature of the phase transition at 155 K, two normal heat capacity curves were determined below and above 155 K by performing a least squares fitting on the measured heat capacities in the regions of 6 − 70 K and 220 − 250 K, respectively, while assuming the correction factor for intramolecular vibrational frequencies, Debye and Einstein temperatures, and the "A" parameter as free parameters. The obtained normal heat capacity is shown in Figure 2 by solid curves. Figure 2 shows that the heat anomalies below 155 K seem to be on a long tail on the lower temperature side of the largest heat anomaly, although the phase transition is of first order. For this reason, it was hard to separately determine the normal heat capacity below 155 K for each anomaly. A single normal heat capacity was assumed, accordingly.

Excess heat capacities obtained by subtracting normal heat capacity from the experimental data are plotted in Figure 4.

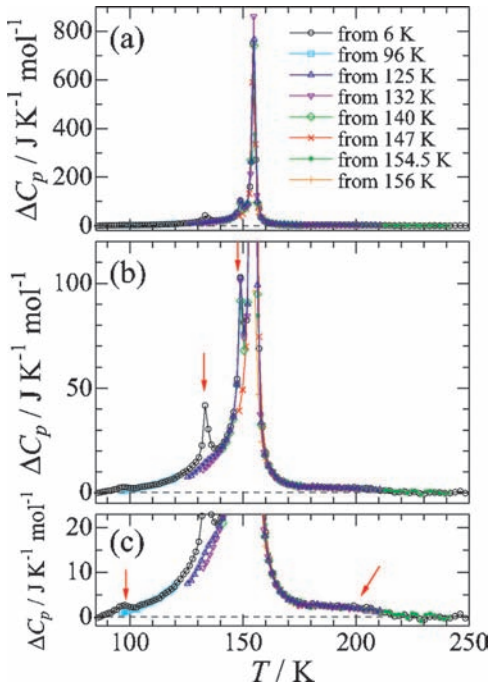

Figure 4. Excess heat capacities of $[Hdamel]_2[Cu^{II}(tdpd)_2]\cdot 2THF$ (a−c). Different colors distinguish data measured from different starting temperatures. Arrows indicate the locations of heat anomalies.

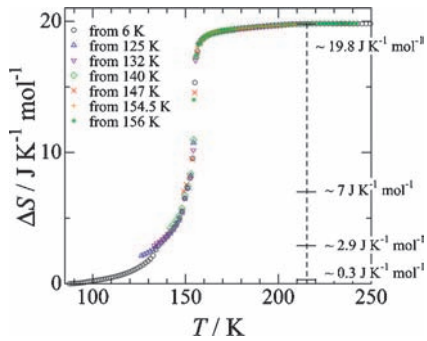

Figure 5. Excess entropies calculated by integration of the excess heat capacities. Different colors distinguish those determined from data with different starting temperatures.

The temperature region associated with the four heat anomalies seems to be over the temperature range from 80 to 220 K. The four phase transitions are located at 97, 134, 149, and 155 K. A long tail is observed from 166 to 220 K for the last one. Figure 4 also shows excess heat capacity (ΔC_p) curves determined from different measurement runs. In reality, the differences are in starting temperatures after cooling from the higher temperature side. Each ΔC_p curve clearly shows a supercooling phenomenon. Each heat anomaly is thus ascribed to phase transitions of first order, as mentioned above. The distinctions are also clearly seen in temperature dependences of entropy obtained by numerical integrations of $\Delta C_p T^{-1}$ against T assuming their coincidence at 180 K (see Figure 5). The dependences on starting-temperature suggest the presence of some polymorphs around the temperature region of the phase transitions. The phases and polymorphs observed by any measurements might, thus, strongly depend on the thermal history of the sample used. By this reason, it can be said that a structural analysis is hard on intermediate phases, although the previous work reported the crystal structure at 140 K.[24]

Numerical integration of the excess heat capacities was carried out from 80 to 220 K, yielding the total enthalpy and entropy

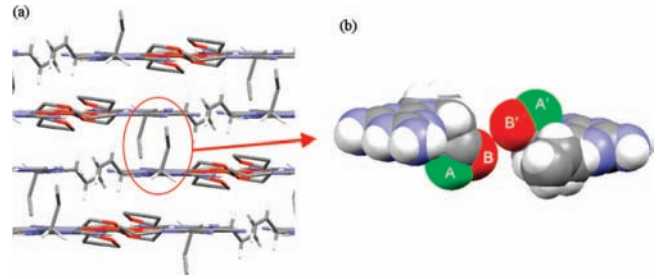

Figure 6. (a) Crystal structure of $[Hdamel]_2[Cu^{II}(tdpd)_2]\cdot 2THF$ at room temperature.[24] (b) Structure of adjacent $[Hdamel]^+$ units at room temperature.[24] A and B denote two conformations of the out-of-plane allyl group of the $[Hdamel]^+$ unit reported at room temperature.

of transition. The temperature dependence of the excess entropy is shown in Figure 5. The combined enthalpy and entropy of transitions were determined to be $\Delta_{trs}H = (2.96 \pm 0.01)$ J mol^{-1} and $\Delta_{trs}S = (19.8 \pm 0.1)$ J K^{-1} mol^{-1}, respectively. The combined entropy of transition thus determined is smaller than $4R$ ln 2 ($\approx$23.1 J K^{-1} mol^{-1}, R = gas constant) expected from the orientational disorders of the two $[Hdamel]^+$ and the two uncoordinated THF seen in the crystal structure at room temperature.[24] The smallness of $\Delta_{trs}S$ suggests that the orientations are restricted for the THF molecules and/or the allyl group of $[Hdamel]^+$.

The previous X-ray study at room temperature suggested that the only restriction on the orientation of the uncoordinated THF is the hydrogen bond to the $[Hdamel]^+$ unit.[24] In other words, there is no restriction on the axial reorientation around the hydrogen bond. This leads to $2R$ ln 2 as the plausible contribution of THF to the excess entropy.

On the other hand, one of the two allyl groups of the $[Hdamel]^+$ unit, which protrudes out of the molecular plane, is close to another one in the adjacent layer as shown in Figure 6a. This out-of-plane allyl group is reported to be disordered in two conformations (A and B) as shown in Figure 6b. Four combinations [(A, A′), (A, B′), (B, A′) and (B, B′)] are, in principle, possible for two out-of-plane allyl groups of two neighboring $[Hdamel]^+$ units. However, it is probably difficult for the adjacent out-of-plane allyl groups to take the (B, B′) orientation, because of strong steric hindrance between them. That is, the energy of the configuration (B, B′) is much higher than those of the other three configurations. Consequently, the available configurations are limited to three, and then the entropy change associated with the orientational disordering is expected to be $\Delta S = R$ ln 3 ($\approx$9.13 J K^{-1} mol^{-1}). This expectation is supported by the combined entropy of transition 19.8 J K^{-1} mol^{-1}. The subtraction of the contribution of THF ($2R$ ln 2 $\approx$ 11.6 J K^{-1} mol^{-1}) yields 8.2 J K^{-1} mol^{-1}, which is reasonably close to R ln 3.

To ensure this thermodynamic consideration, we re-examined the crystal structure of $[Hdamel]_2[Cu^{II}(tdpd)_2]\cdot 2THF$ by X-ray at 200 K, where the complex is still in the room-temperature phase. The structure refinement assuming the disorder of the carbon atom of the out-of-plane allyl group was carried out and converged successfully with the carbon atom occupying A and B sites with the ratio 3:1. The resultant structure of $[Hdamel]^+$ is depicted in Figure 7. Considering the possible combinations of the conformations, the (A, A′) configuration should be the lowest energy level. On the other hand, the (B, B′) configuration is the highest in energy with a large energy gap from the others because of the severe steric hindrance. The configurations (A, B′) and (B, A′) degenerate with the same energy beyond the (A, A′) configuration. The situation is depicted in Figure 8 as

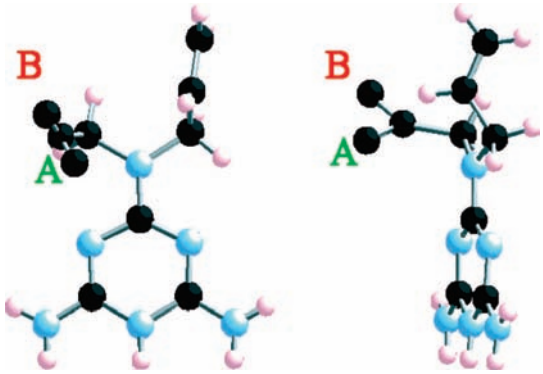

Figure 7. Molecular structures of the $[Hdamel]^+$ unit of $[Hdamel]_2[Cu^{II}(tdpd)_2]\cdot 2THF$ determined by X-ray structure analysis at 200 K. A and B denote two conformations of the out-of-plane allyl group of $[Hdamel]^+$ unit.

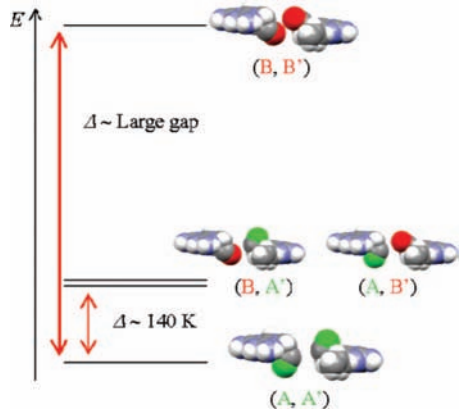

Figure 8. Energy diagram of the four configurations of the conformation of the neighboring $[Hdamel]^+$ pair.

an energy diagram. Because the (B, B′) configuration is expected to be much higher in energy, the situation can be mapped to be a so-called two-level system. From the experimental ratio 3:1, the relative occupancies of (A, A′), (A, B′) and (B, A′) configurations are deduced as 1, 1/2, and 1/2, respectively. The energy gap is then estimated to be about 140 K assuming Boltzmann distribution, while ignoring the highest level (B, B′). The expected entropy change associated with the disordering process is slightly smaller than R ln 3 that corresponds to the total entropy change at the high temperature limit. The configurational entropy at 220 K is calculated to be 8.7 J K^{-1} mol^{-1} while assuming the two-level system. This yields the total entropy change of 20.2 J K^{-1} mol^{-1} from the contributions of the allyl groups (ΔS = 8.7 J K^{-1} mol^{-1}) and the THF (ΔS = 2R ln2). This total entropy change is favorably compared with the experimental one, ΔS = 19.8 J K^{-1} mol^{-1}.

The temperature dependence of the entropy shows four plateaus corresponding to the phase transitions. The entropy changes from 80 K to the plateaus are 0.3, 2.9, 7, and 19.8 J K^{-1} mol^{-1} (total entropy change). The first is much smaller than R ln 2 (≈ 5.8 J K^{-1} mol^{-1}). The second corresponds to a half of R ln 2, and the third is in between R ln 2 and R ln 3. The previous structural investigation[24] showed a possible formation of superstructure(s). The superstructures can be consistent with partial disordering, leading to nonrational entropy plateaus. It is, however, hard to propose the disordering process corresponding to those entropy change at present because of the lack of experimental information even for reliable lattice parameters. To establish the disordering process in detail, it is necessary to determine the crystal structures of the intermediate and the most stable phases under precise temperature-control on the sample having the definite thermal history. These structural issues are left for future work.

IV. Conclusions

The heat capacity of $[Hdamel]_2[Cu^{II}(tdpd)_2]\cdot 2THF$ was measured from 6 to 250 K. The four heat anomalies observed around 150 K were associated with the disordering of the orientations of the uncoordinated THF molecules and the out-of-plane allyl groups of $[Hdamel]^+$ units. The quantitative analysis of the entropy change of the phase transition revealed the presence of the strong correlation between the dynamics of the adjacent allyl groups. The analysis should be regarded as another example demonstrating the unique capability of thermal study based on the statistical mechanics. Although the information on the time scale involved is often missing in thermodynamic discussion (this is also the case for the present result), the existence of such a correlation can be detected in "entropy" without assuming special models.[23] As the "dynamical" structure of molecules is crucial to tune functionality of condensed systems,[30] the present result would contribute to the rational design of inorganic complex materials.

Acknowledgment. This work was supported in part by the Yamada Science Foundation (K. S. and Y. Y.) and by Grant-in-Aid for Priority Area "Chemistry of Coordination Space" (No. 18033004 and 18033031) from the Ministry of Education, Culture, Sports, Science and Technology, Japan (K. S. and S. K.).

Supporting Information Available: X-ray crystallographic information for compound 1 (CIF format). This material is available free of charge via the Internet at http://pubs.acs.org.

References and Notes

(1) Lehan, J.-M. *Supramolecular Chemistry; Concepts and Perspectives*; VCH Publications: Weinheim, 1995.
(2) Matsuda, R.; Kitaura, R.; Kitagawa, S.; Kubota, Y.; Belosludov, R. V.; Kobayashi, T. C.; Sakamoto, H.; Chiba, T.; Takata, M.; Kawazoe, Y.; Mita, Y. *Nature* **2005**, *436*, 238.
(3) Kitagawa, S.; Kawata, S. *Coord. Chem. Rev.* **2002**, *224*, 11.
(4) Kitagawa, S.; Kitamura, S.; Noro, S. *Angew. Chem. Int. Ed.* **2004**, *43*, 2334.
(5) Kitagawa, S.; Uemura, K. *Chem. Soc. Rev.* **2005**, *34*, 109.
(6) Rowsell, J. C.; Yaghi, O. M. *Angew. Chem. Int. Ed.* **2005**, *44*, 4670.
(7) Kahn, O. *Molecular Magnetism*; VCH Publications: New York, 1993.
(8) Miller, J. S.; Epstein, A. J. *Coord. Chem. Rev.* **2000**, *206–207*, 651.
(9) Gütlich, P.; Goodwin, H. A. Spin Crossover in Transition Metal Compounds. *Top. Curr. Chem.* **2004**, 233–235.
(10) Gütlich, P.; Garcia, Y.; Goodwin, H. A. *Chem. Soc. Rev.* **2002**, *29*, 419.
(11) Oshio, H.; Nakano, M. *Chem. Eur. J.* **2005**, *11*, 5178.
(12) Yamashita, M.; Ishii, T.; Hiroyuki, M. *Coord. Chem. Rev.* **2000**, *198*, 347.
(13) Kitagawa, H.; Mitani, T. *Coord. Chem. Rev.* **1999**, *190–192*, 1169.
(14) Kobayashi, A.; Fujiwara, E.; Kobayashi, H. *Chem. Rev.* **2004**, *104*, 5243.
(15) Ye, Q.; Wang, X. S.; Zhao, H.; Xiong, R. G. *Chem. Soc. Rev.* **2005**, *34*, 208.
(16) Okubo, T.; Kawajiri, R.; Mitani, T.; Shimoda, T. *J. Am. Chem. Soc.* **2005**, *127*, 17598.
(17) Leininger, S.; Olenyuk, B.; Stang, P. *J. Chem. Rev.* **2000**, *100*, 853.
(18) Seidel, S. R.; Stang, P. J. *Acc. Chem. Res.* **2002**, *35*, 972.
(19) Ockwig, N. W.; Delgado-Friedrichs, O.; O'Keeffe, M.; Yaghi, O. M. *Acc. Chem. Res.* **2005**, *38*, 176.
(20) Fujita, M.; Tominaga, M.; Hori, A.; Therrien, B. *Acc. Chem. Res.* **2005**, *38*, 369.
(21) Miyazaki, Y.; Wang, Q.; Sato, A.; Saito, K.; Yamamoto, M.; Kitagawa, H.; Mitani, T.; Sorai, M. *J. Phys. Chem. B* **2002**, *106*, 197.

(22) Ikeuchi, S.; Saito, K.; Nakazawa, Y.; Sato, A.; Mitsumi, M.; Toriumi, K.; Sorai, M. *Phys. Rev. B* **2002**, *66*, 115110.

(23) Saito, K.; Yamamura, Y. *Thermochim. Acta* **2005**, *431*, 21.

(24) Adachi, K.; Sugiyama, Y.; Yoneda, K.; Yamada, K.; Nozaki, K.; Fuyuhiro, A.; Kawata, S. *Chem. Eur. J.* **2005**, *11*, 6616.

(25) Yamamura, Y.; Saito, K.; Saitoh, H.; Matsuyama, H.; Kikuchi, K.; Ikemoto, I. *J. Phys. Chem. Solids* **1995**, *56*, 107.

(26) Sheldrick, G. M. *SHELXL97*, University of Göttingen; Germany, 1997.

(27) Cadioli, B.; Gallinella, E.; Coulombeau, C.; Jobic, H.; Berthier, G. *J. Phys. Chem.* **1993**, *97*, 7844.

(28) Frisch, M. J.; Trucks, G. W.; Schlegel, H. B.; Scuseria, G. E.; Robb, M. A.; Cheeseman, J. R.; Montgomery, J. A.; Vreven, Jr., T.; Kudin, K. N., Burant, J. C.; Millam, J. M.; Iyengar, S. S.; Tomasi, J.; Barone, V.; Mennucci, B.; Cossi, M.; Scalmani, G.; Rega, N.; Petersson, G. A.; Nakatsuji, H.; Hada, M.; Ehara, M.; Toyota, K.; Fukuda, R.; Hasegawa, J.; Ishida, M.; Nakajima, T.; Honda, Y.; Kitao, O.; Nakai, H.; Klene, M.; Li, X.; Knox, J. E.; Hratchian, H. P.; Cross, J. B.; Bakken, V.; Adamo, C.; Jaramillo, J.; Gomperts, R.; Stratmann, R. E.; Yazyev, O.; Austin, A. J.; Cammi, R.; Pomelli, C.; Ochterski, J. W.; Ayala, P. Y.; Morokuma, K.; Voth, G. A.; Salvador, P.; Dannenberg, J. J.; Zakrzewski, V. G.; Dapprich, S.; Daniels, A. D.; Strain, M. C.; Farkas, O.; Malick, D. K.; Rabuck, A. D.; Raghavachari, K.; Foresman, J. B.; Ortiz, J. V.; Cui, Q.; Baboul, A. G.; Clifford, S.; Cioslowski, J.; Stefanov, B. B.; Liu, G.; Liashenko, A.; Piskorz, P.; Komaromi, I.; Martin, R. L.; Fox, D. J.; Keith, T.; Al-Laham, M. A.; Peng, C. Y.; Nanayakkara, A.; Challacombe, M.; Gill, P. M. W.; Johnson, B.; Chen, W.; Wong, M. W.; Gonzalez, C.; Pople J. A. *Gaussian 03*, Rev. D.02; Gaussian, Inc., Wallingford CT, 2004.

(29) Kittel, C. *Introduction to Solid State Physics*; John Wiley & Sons, Inc.: New York, 2004.

(30) Akutsu, H.; Saito, K.; Sorai, M. *Phys. Rev. B* **2000**, *61*, 4346.

JP710936Q